Clinical Case Reports International

Research Article
Published: 15 Sep, 2023

Kinetics, Thermodynamics and Adsorption Studies of Copper Azithromycin Complex for Removal of Toxic New Fuchsin Dye from Wastewater

Ibrahim SM, Mohamed NS and Ahmed MM*

Department of Chemistry, New Valley University, Egypt

Abstract

The current study aims to investigate the interaction of the antibiotic Azithromycin (Az) as a ligand with copper (II) metal and its efficiency in the removal of toxic New Fuchsin (NFD) dye from wastewater. The suggested structure of was characterized by different techniques such as FTIR, UV-Vis, mass spectrometry, and elemental analysis. The efficacy of using Copper-Azithromycin complex (Cu2+-Az) complex to remove New Fuchsin (NFD) dye from aqueous solution was investigated through batch adsorption studies and examined using spectroscopic UV-Vis techniques. The effects of the contact time, the initial concentration, the temperature, and the adsorbent dosage are studied. The (Cu2+-Az) complex and (Cu2+-Az/NFD) dye are characterized by SEM and FTIR analysis. The removal percentage of dye increase with increase the adsorbent dose (78.2%) as well as increase with an increase in the initial dye concentration. Adsorption equilibrium data was fitted with Langmuir and Freundlich equations to describe the isotherms.

Keywords: Cu-azithromycin complex; New Fuchsin dye; Kinetic parameters; Spectral studies

Introduction

The discovery of azithromycin, a macrolide, in the 20th century was incredibly significant, and it was used as an example of biomedicine and drug design [1]. Azithromycin is a broad-spectrum antibacterial drug that belongs to the second generation of the macrolide class. In recent years, it has garnered a growing amount of interest due to its extra effects on host-defense responses and chronic human disorders. It was first synthesized in the early 1980s as a semi-synthetic derivative of erythromycin, and it has a 15-membered lactone ring as its prototype azalide structure. Pfizer researchers in the United States made the discovery about the same time it was made public [2]. The antibacterial properties of azithromycin are effective against a wide range of microorganisms that cause disease. It has been shown to be effective in treating a variety of diseases, and the curative impact is noticeable. But a significant amount of effluent was released into the environment throughout the manufacturing process [3], given its antiviral and immunomodulatory action together with its well-established safety profile, it has been suggested as a possible therapeutic for the treatment of SARS-CoV-2 pneumonia [2,4,5]. The antibiotic azithromycin has a large molecular weight and includes reactive centers like N atoms, aromatic rings, and C=O, all of which are regarded to be sites of adsorption on the surface of metals. This compound is an antibiotic of the macrolide class, and it is used in the treatment of a wide range of bacterial infections [2,6]. Azithromycin contains an amino group (-RC=N-), N and O donor atoms, which have been proven to exhibit a broad variety of biological activities and physicochemical features, such as metal complexation. Copper is a valuable metal because it can be put to use in a wide variety of applications, both in the commercial and consumer sectors of the economy. Copper not only has favorable thermal and mechanical properties, but it also has antibacterial action [6-8]. Previous research on the interaction of azithromycin with copper (II) ion and other research both indicate azithromycin's affinity for metal cations. All of these electropositive species are classified as Lewis's acids, and they have a strong interaction with Lewis bases. Lewis bases are distinguished from other types of molecules by the presence of accessible lone pairs that decorate their molecules [9-11].

Over the course of the last several years, there has been a steady increase in focus placed on the difficulties associated with environmental concerns. One of these issues is the pollution of wastewater by industrial organic chemicals including paper, cosmetics, plastics, food, synthetic detergents, dyes and textiles [12]. Due to the widespread use of organic dyes in a variety of industrial

OPEN ACCESS

Correspondence:
Samia M Ibrahim, Department of Chemistry, New Valley University, El-Kharga 72511, New Valley, Egypt

Received Date: *21 Aug 2023*
Accepted Date: *11 Sep 2023*
Published Date: *15 Sep 2023*

Citation:
Ibrahim SM, Mohamed NS, Ahmed MM. Kinetics, Thermodynamics and Adsorption Studies of Copper Azithromycin Complex for Removal of Toxic New Fuchsin Dye from Wastewater. Clin Case Rep Int. 2023; 7: 1609.

processes and their subsequent release into the environment, organic dyes are often found as pollutants in wastewater. The majority of the dyes are refractory, colorants, and some of them even have the potential to be carcinogenic and poisonous. Because dyes can have detrimental effects on human health as well as ecosystems, scientists have been working to develop dye wastewater treatment methods that are both simple and effective [13]. This contamination has evolved into a significant problem due to the fact that the discharge of dyes into the environment caused by a variety of human and industrial activities can, in the absence of appropriate treatment, pose a significant risk to both the health of humans and the aquatic environment [14,15]. New Fuchsin (NF), in particular, is one of the key dyes that are used for staining collagen, muscle mitochondria, and tubercle bacillus, as well as biological stains, paper, leather, and cotton coloring agents. It is also one of the most extensively used dyes [16-18]. New Fuchsin (NFD), also known as the new fuchsin or magenta (III) dye, is a green-colored organic solid chemical that is employed as a dye of the triarylmethane class. Before being released into the environment, NF must first be eliminated from all waterways and wastewaters because of its slow rate of biodegradation, toxicity, and carcinogenicity [19,20]. Because of this, it is very necessary to either remove this dye from wastewater or treat it in order to lessen the negative effects it has on both the environment and human health. In order to treat wastewater that contains organic dyes, several different treatment techniques have been used, including physical methods (filter, precipitation, and coagulation-flocculation) [21-24], biological methods (microorganisms and enzymes), and chemical approaches (oxidation, electrolysis and ozonation) [25,26]. Regrettably, studies have revealed that the removal of dyes using these methods is either non-destructive or ineffective [27]. Adsorption is one of the promising strategies for treating wastewater owing to its cheap cost, simplicity, and ease of processing at commercial scale and it has attracted a substantial amount of attention [28-30]. Again, we succeed to use Az as adsorbent in the removal of toxic New Fuchsin dye from wastewater [31]. The main objectives of this study are (1) to synthesis copper (II)-azithromycin complex and characterized through elemental analysis, FT-IR, and mass spectroscopy and (2) to investigate its ability for removal of dye New Fuchsin as well as the effects of different parameters such as contact time, initial dye concentration, adsorbent dose, and temperature were investigated. The removal rate kinetics and isotherms for New Fuchsin adsorption onto copper complex were also studied, and the characterization of copper complex as an adsorbent is presented.

Experimental

Materials and methods

Azithromycin ligand used in our work was obtained from Century Pharmaceuticals LTD., India. Copper complex adsorbent was synthesized according to the general complexation method. New Fuchsin dye ($C_{22}H_{24}N_3Cl$) (Basic Violet 2) was used without further purification. Its molecular weight, Color Index (C.I.) and maximum wavelength (λ_{max}) are: 365.9 g mol^{-1}, 42520 and 547 nm, respectively. The stock solution of (NFD) (1000 mg.L^{-1}) was prepared and the dye solution used for the experiments was prepared by diluting the stock solution as needed. Absorbance was measured using 1 cm route length cells and a program controller on a Perkin Elmer Lambda 750 that records UV/Vis spectra. To hasten the process, a centrifuge (FRONTIERTM 5000 SERIES MULTI, OHAUS) was used. Throughout the whole of the investigation, analytical grade materials were used. FTIR spectra were recorded by using NICOLET-6700 FTIR Thermo Electron Corporation spectrophotometer in the range of (4000-400) cm^{-1}. Elemental analysis (C, H and N) was carried out on an Automatic analyzer CHNS-Vario EL III-Elemental Germany. Mass spectra of ligand and complex were recorded using GCMS-QP2010 plus Japan spectrophotometer. The surface morphology was observed using a JSM5400LV Scanning electron microscope.

Synthesis of (Cu^{2+}-Az) complex

The copper complex was synthesized by the general method [32]. The equimolar amount of ligand (Az) and metal (Cu (II)) were dissolved separately in 20 ml of each of ethanol and distillated water, respectively. Both the solutions were mixed together and stirred at room temperature for 60 min in alkaline medium, then the precipitate of the complex was filtered and washed with an excess of ethanol and finally dried at room temperature through 24 h. This newly synthesized complex is violet colored solid, stable at room temperature and insoluble in common solvents such as ethanol, methanol, chloroform and ethyl acetate but sparingly soluble in DMF and DMSO. Yield 0.26 gm (22.4%), decomposition temperature 178°C to 180°C. Elemental analysis, Calculated: C, 55.19; H, 8.57; N, 3.22. Observed: C, 54.48; H, 9.16; N, 3.31.

Results and Discussion

In this part, we synthesis complex of Copper-Azithromycin (Cu^{2+}-Az) and using it as an adsorbent to study its efficiency for the removal of toxic New Fuchsin dye. In order to comprehend the adsorption process, equilibrium and kinetic data from batch adsorption experiments were compiled. The influence of adsorption factors such as adsorbent dose, contact time, initial dye concentration, and temperature was also reported. Analysis as FTIR, Mass, elemental analysis techniques were studied for the Azithromycin (Az) and the synthesized complex (Cu^{2+}-Az) complex as well as SEM and UV-Vis spectrophotometer technique were also studied for the (NFD) dye and (Cu^{2+}-Az/NFD).

FTIR analysis of (Az), (Cu^{2+}-Az) complex and ($Cu2^{+}$-Az/NFD)

Azithromycin has a high number of lone pair rich sites and amine substituted lactone ring to form complexes with metals than other antibiotics [1]. The complexation reaction is confirmed through the FTIR spectra of free azithromycin ligand and copper complex, as illustrated in Figure 1. The spectra of (Az) showed that the vibrational modes of C-C, C-O, symmetric C-N, and asymmetric C-N that located at 994, 1051, 1083, and 1187 cm^{-1}, respectively. The vibrational modes of the five Methylene (CH_2) groups were measured at the following frequencies: 2935, 2830, 1378, 1254, 796, and 574 cm^{-1}, respectively: υ_{as} (CH_2), υ_{a} (CH_2), δ_{sciss} (CH_2), δ_{rock} (CH_2), δ_{wag} (CH_2), and δ_{twist} (CH_2). The vibrational modes of the 14 methyl groups have been ascribed to the bands that were found at 2971, 2892, 1456, and 834 cm^{-1}, and these modes are referred to as υ_{as} (CH_3), υ_{s} (CH_3), δ_{rock} (CH_3), and δ_{wag} (-CH_3), respectively. It is possible that the vibrations of symmetric and asymmetric C=O are responsible for the bands that were found at 1720 and 1653 cm^{-1}, respectively. The vibrational modes of out-of-plane bending, in-plane bending, and stretching vibrations of -O-H bonds were assigned to the bands with wave numbers at 731 cm^{-1}, 898 cm^{-1}, and 3245 cm^{-1} to 3490 cm^{-1}, respectively [33]. In copper complex, FTIR spectra were recorded to establish the structure of the complex and to find out where the ligand can be coordinated in the complex. Table 1 presents the frequency distributions of the ligand and copper

Table 1: Infrared spectral data (wave number ú) cm^{-1} for the ligand and its copper complex.

Compound	v (O-H)	v (C=O) Lactone	v (C-O) alkyl aryl ether	v (C-N) asy.	v (C-N) sym.	v (C-C)	v (M-N)	v (M-O)
Az	3490 (sh) 3562 (w)	1720 (sh)	1051 (sh)	1187 (m)	1083 (sh)	994		
(Cu $AzC_2H_3O_2$)	3433 (b)	1719 (sh)	1006 (w)	1177 (sh)	1056 (w)	961	571 (m)	462 (m)

Table 2: Results of various isotherm plots for the adsorption of (NFD) dye onto (Cu^{2+}-Az) complex at 547 nm.

Models	Isotherm constants			Correlation
Langmuir	q_m=0.0061 mg/g	K_L= 23187.33 L/mg	R_L=0.775	0.999
Freundlich	n=0.29	K_F= 84.18		0.972

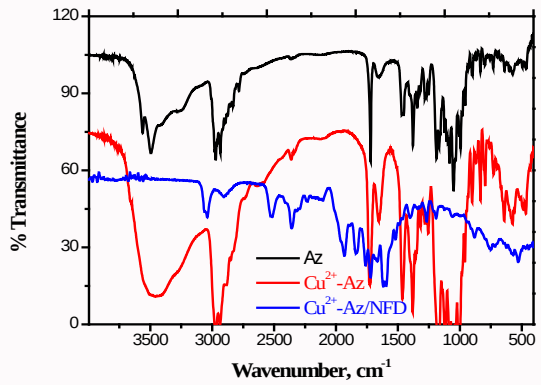

Figure 1: FTIR spectra of Az, (Cu^{2+}-Az) complex and (Cu^{2+}-Az/NFD).

complex in their typical forms. Two distinct bands, located at 3490 and 3562 cm^{-1} on the FT-IR spectra of the free ligand (Az), have been attributed to stretching vibrations of -O-H. On complexation, these bands changed to one broad band and shifted to lower frequency for the copper complex and appeared at 3433 cm^{-1}, indicating coordination through the oxygen atom (O-H→M) with the metal ion. The spectral data of the prepared complex records the characteristic frequencies bands of asymmetric C-N, symmetric C-N, C-O, and C-C stretching vibration for the group at 1177 cm^{-1}, 1056 cm^{-1}, 1006 cm^{-1} and 961 cm^{-1}, respectively, the lower frequency value of asymmetric C-N in the complexes indicated that the monodentate binding nature of the tertiary amine group (N-R_3). The (M-N) and (M-O) vibrations have been assigned, respectively, to two additional weak bands that have been discovered in the lower frequency area. These bands were observed at 571 cm^{-1} and 462 cm^{-1}. [34-37]. The FTIR spectra of the (Cu^{2+}-Az) complex after the (NFD) adsorption was obtained in order to get an understanding of the nature of the interaction that occurs between the (Cu^{2+}-Az) complex and the new fuchsin dye (NFD). It shows completely different bands from the (Cu^{2+}-Az) complex as well as some bands have been shifted in the position to lower wavelength with low intensities as shown in Figure 1. This difference indicates that there are interaction occurred between the complex and the dye.

Mass spectra

In the spectrum of Azithromycin (Az) ligand; Figure 2, the molecular ion peak was observed at m/z 749 which is equivalent to its molecular weight ($C_{38}H_{72}N_2O_{12}$). This molecular ion undergoes fragmentation with loss of ($C_8H_{15}O_6$) to give a species $C_{30}H_{57}N_2O_9$- at 590 m/z and other peaks at 413, 374, 158, 116 and 98 amu for $C_{22}H_{39}NO_6$, $C_{20}H_{40}NO_5^+$, $C_9H_{20}NO^+$, $C_6H_{14}NO^+$ and $C_6H_{12}N^{+3}$ respectively, Scheme (I). As shown in Figure 3, the molecular ion peak of Cu (II) complex was observed at 871 m/z, which is equivalent to its suggested molecular weight ($C_{40}H_{74}CuN_2O_{14}$). This molecular ion undergoes fragmentation with loss of (-OCH_3) molecule to give a species $C_{39}H_{72}CuN_2O_{13}$ at 841 m/z. On the other hand, there are peaks at 824, 633, 158 and 116 for $C_{39}H_{71}CuN_2O_{12+}$, $C_{32}H_{60}N_2O_{10}$, $C_9H_{20}NO^+$ and $C_6H_{14}NO^+$ respectively, as shown in Scheme (II).

Batch adsorption studies

Batch experiments were carried out in order to investigate the effects of the initial adsorbate concentration, the adsorbent dose, the time of adsorption and the temperature on the adsorption studied. The (NFD) dye sample was prepared by dissolving a properly weighed quantities of dye in 1 liter of distill water to yield 1,000 parts per million of (NFD) dye. In order to get the desired concentration, the stock solution was diluted. In every single trial, we started with freshly prepared dilutions. Specific quantity of (NFD) dye solution of a known Concentration (Co) was mixed with a required amount of the adsorbent and was shacked for different time duration and centrifuged for 10 min at 2000 rpm. After centrifugation, the solution was then filtered using a filter paper and analyzed to determine the remaining concentrations of (NFD) dye in the filtrate using UV-visible spectrophotometer at wavelength of 547 nm.

Studies of equilibrium and kinetic

In order to achieve the desired concentration, a stock solution of dye (NFD) was first subjected to further dilution. The following variables were investigated: the concentration of dye (40 mg L^{-1}), temperature (303-333°K), contact duration (2-12 min), and (Cu^{2+}-Az) complex adsorbent (10 mg). Following each repetition of the experiment about the removal conditions, the dye solutions, and the adsorbents were subjected to centrifugation (2000 rpm for ten minutes). At a wavelength of 547 on a UV-Vis spectrophotometer, the amounts of dye molecules that were still present in solution were analyzed. We calculated the elimination efficiency as part of the kinetic investigation that we were doing. Equations were used to determine the removal effectiveness (qe, in %) and the adsorption capacity (qc, in mg g^{-1}), respectively, both (1) and (2) in their own right [38,39].

$$q_c = \frac{(C_0 - C_e)V}{m} \quad (1)$$

$$q_e = \frac{(C_0 - C_e)}{C_0} \times 100 \quad (2)$$

Where C_e and C_0 (mg L^{-1}) are the concentrations of the dyes in the liquid phase at the equilibrium and initial, respectively. In this equation, V represents the volume of the solution in liters, and m is the quantity of adsorbent that was applied (g). Every experiment was performed with three separate replicates, and the mean results were taken into account in the statistical analysis.

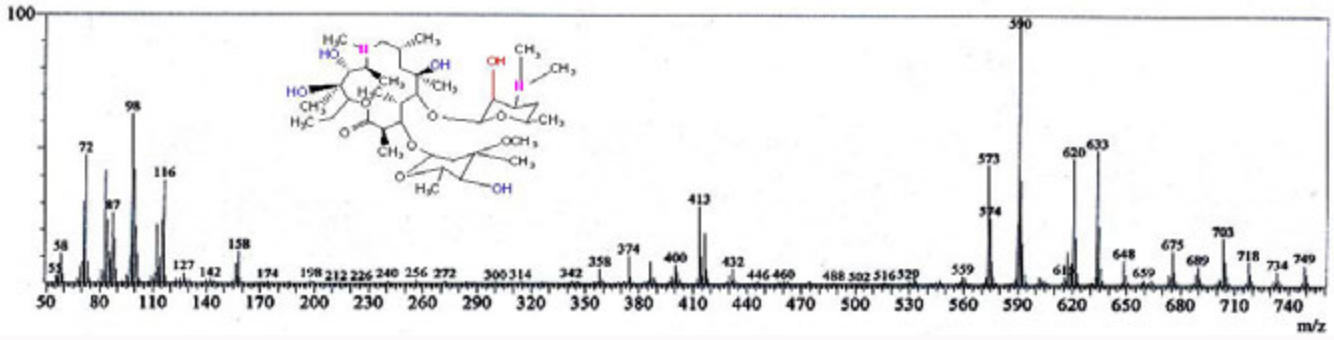

Figure 2: Mass spectrum of Azithromycin (Az) ligand.

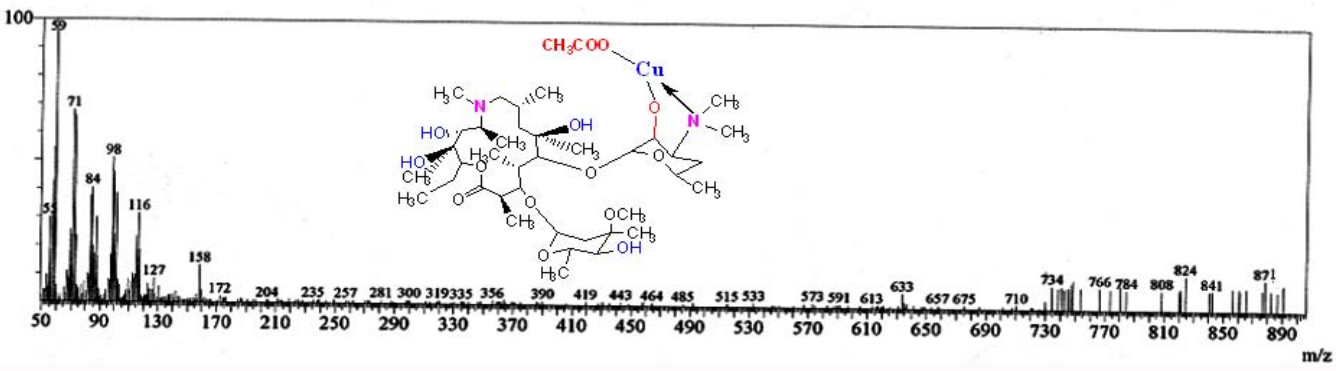

Figure 3: Mass spectrum of ($CuAzC_2H_3O_2$) complex.

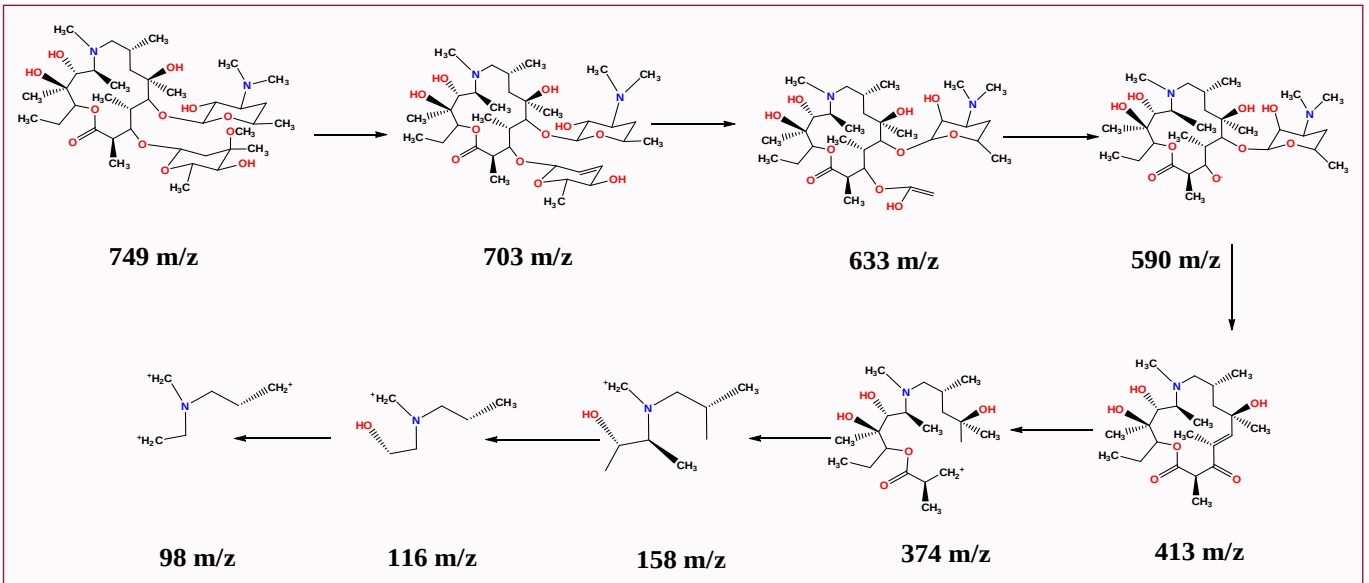

Scheme I: Fragments of Azithromycin (Az) Ligand.

Adsorption isotherm

Langmuir isotherm: Langmuir's isotherm may be used to compute equilibrium sorption if the surface in question contains a limited number of sites that are similar to one another. The expression may also be written as follows [40]:

$$\frac{1}{q_c} = \frac{1}{q_m} + \frac{1}{K_L q_m C_e} \quad (3)$$

The form of this isotherm may also be described in terms of the separation factor, which is denoted by the notation (R_L) [41], which reads as follows:

$$R_L = \frac{1}{1 + K_L C_0} \quad (4)$$

In this context, K_L refers to a Langmuir constant, which is measured in units of mg/L and is associated with sorption affinity as well as the free energy of binding. In this instance, q_c refers to the

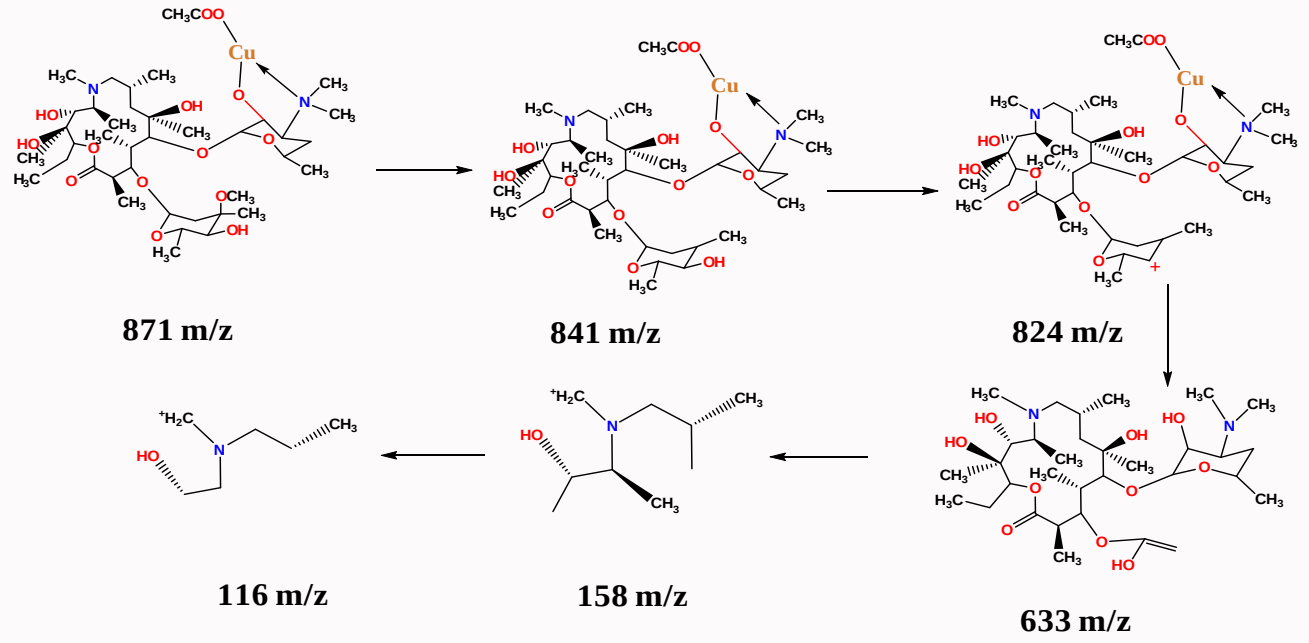

Scheme II: Fragments of (Cu^{2+}-Az) complex.

concentration of dye that has reached equilibrium on the biosorbent (mg/g). The concentration of the dye that is at equilibrium in a solution is denoted by the symbol C_e (mg/l). When a monolayer forms on a bio-sorbent, the concentration of dye at that point is denoted by the symbol q_m (mg/g).

Freundlich isotherm: The equation for the Freundlich method, which is used to analyses the energy of heterogeneous surface systems, is provided by [41,42]:

$$\ln q_c = \ln K_f + \frac{1}{n}\ln C_e \qquad (5)$$

Where the Freundlich constants, K_F and n, are determined by the relationship between the natural logarithms of q_c and C_e. Both the system's sorption capacity and its sorption intensity are connected to the parameter constants K_f and 1/n, respectively. The value of the term (1/n) magnitude gives an indicator of how favorable the sorbent/adsorbate systems are [43].

SEM analysis

SEM analysis was used to determine the morphology of both the synthesized (Cu^{2+}-Az) complex and the (Cu^{2+}-Az/NFD) samples, as shown in Figure 4. The adsorption process is a surface phenomenon; its success largely depends on the surface features of the adsorbent material, such as the number of pores present on the surface of the material [44]. The adsorbent material (a) (Cu^{2+}-Az) complex has a greater number of pores, larger cavities, granular particles, and nonporous solid material. The (Cu^{2+}-Az) complex was responsible for the absorption of the (NFD) dye, which led to the creation of a layer of (NFD) material on their surface. The microstructure of (Cu^{2+}-Az/NFD) (b) shows a significant change as a consequence of the chemical and physical interaction that occurs between the copper complex adsorbent and adsorbate molecules. From this result, copper complex was shown to have more than adequate features for the elimination of NF dye from aqueous solutions.

Removal of new fuchsin dye

Effect of adsorbent dose and initial dye concentration: Figure 5A, 5B shows the effect of initial dye concentration on adsorption onto the (Cu^{2+}-Az) complex adsorbent. In this experiment the amount of adsorbent was constant 10 mg of (Cu^{2+}-Az) complex in 10 ml of dye solution, while the concentration of dye was varied from 0.2×10^{-4} mol dm^{-3} to 1×10^{-4} mol dm^{-3}. By plotting the adsorption capacity (q_c) against the dye concentration (Figure 5A), it can be seen that

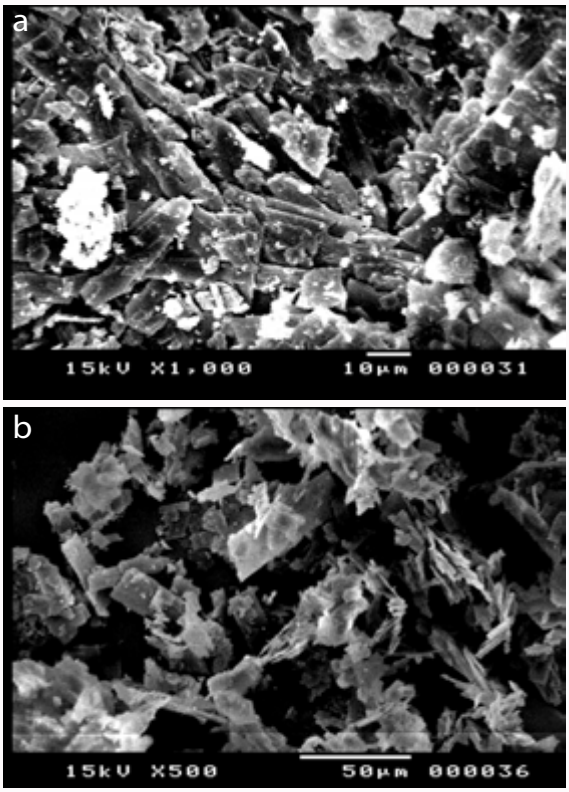

Figure 4: SEM micrographs of a) the complex (Cu^{2+}-Az) complex (before adsorption) and (b) The (Cu^{2+}-Az/NFD) (after (NFD) dye adsorption).

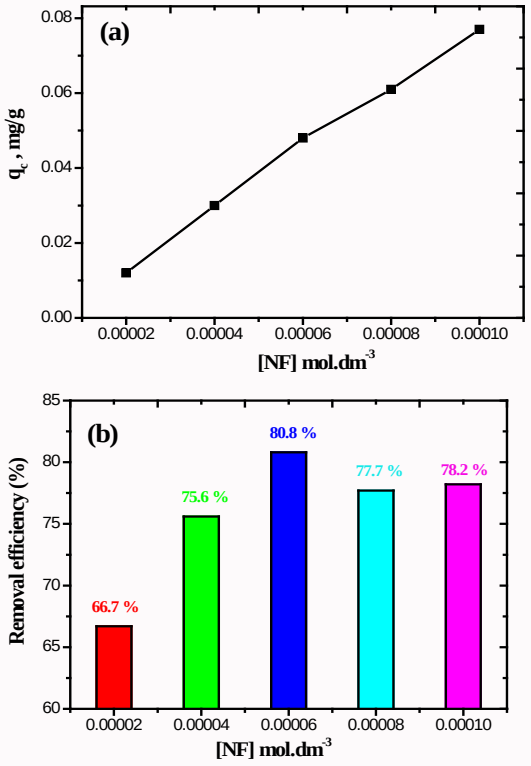

Figure 5: Effect of concentration of dye on (a) adsorption capacity (q_c); (b) removal efficiency in NF removal at 30°C using (Cu^{2+}-Az) complex.

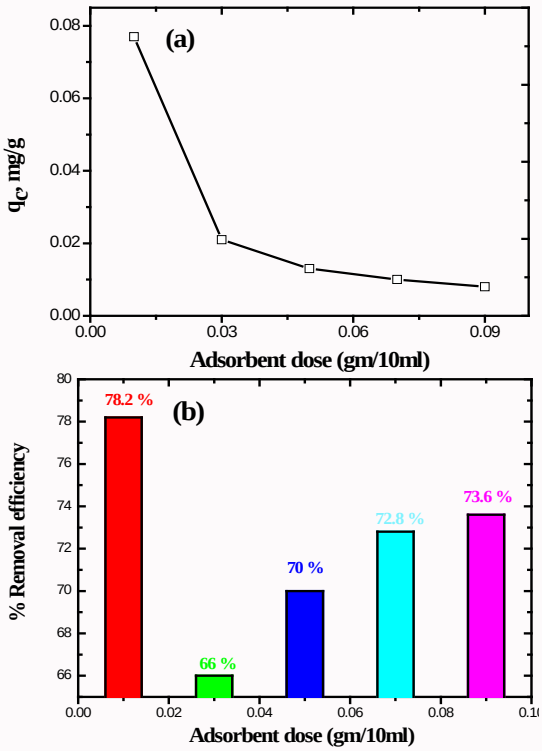

Figure 6: Effect of adsorbent dose on (a) adsorption capacity (q_c); (b) removal efficiency on NF removal in 40 mg/l of dye at 30°C using (Cu^{2+}-Az) complex.

the adsorption capacity of the dye gradually increases with increasing concentration at constant time 10 min. Adsorption capacity increases from 0.012 mg/g to 0.077 mg/g when the concentration of the dye is

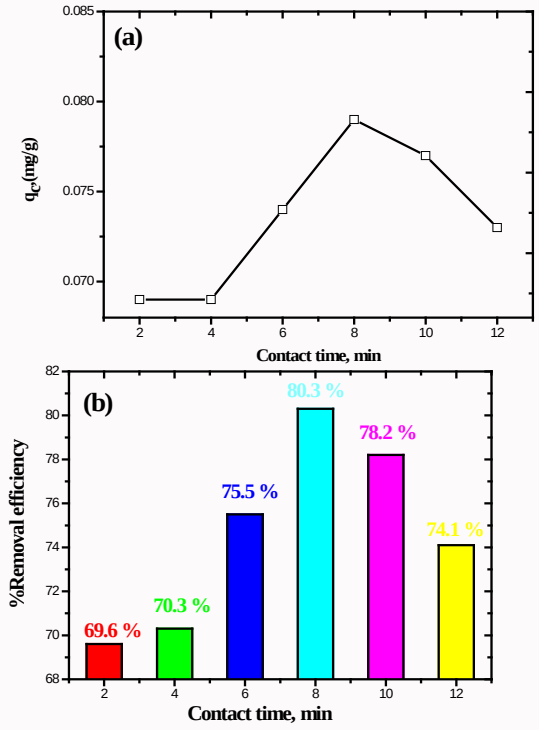

Figure 7: Effect of contact time on: (a) adsorption capacity (q_c) and (b) removal efficiency on NF removal at 30°C using (Cu^{2+}-Az) complex.

changed from 0.2×10^{-4} mol dm^{-3} to 1×10^{-4} mol dm^{-3}. The variation of removal efficiency % versus dye concentration which have a maximum value 80.8% at 0.6×10^{-4} mol dm^{-3} as shown in Figure 5B. Different amounts of the adsorbent dose ranged from 10 to 90 mg/10 ml were tested for this study. The adsorption capacity (q_c) decreased sharply with increasing adsorbent dosage from 0.01 to 0.09 g/10 ml, with a maximum value of 0.077 mg/g, Figure 6A. On the other hand, the percentage removal efficiency of New Fuchsin dye was 78.2% at 0.01 gm of adsorbent dose, then dropped to 66% at 0.03 gm of adsorbent dose, and after that increased with increasing the amount of adsorbent, as shown in Figure 6B.

Influence of contact time: Figure 7A, 7B depicts the influence of contact time on the elimination of (NFD) dye at a concentration of 40 mg/l across a time range of 2 min to 12 min. The adsorption capacity and removal efficiency of the dye increased to reach a maximum value that was 0.079 mg/g and 80.3%, respectively, then decreased with increasing time. The optimum adsorption was achieved in 8 min.

Influence of temperature

The removal efficiency and adsorption capacity of dye increased from 303°K to 323°K with a maximum value of 92.6% and 0.194 mg/g, respectively, and with an increase in temperature, suddenly dropped to achieve the adsorption value of 84.9% at 333°K as shown in Figure 8A, 8B.

Adsorption isotherm: The adsorption potential, binding potential and surface attributes may all be articulated with the use of an adsorption isotherm. Isotherms are used to determine the equilibrium correlation that exists between the adsorbate and the adsorbent when the circumstances are at their best. The adsorption behavior may be analyzed using a number of different theoretical models; however, for the sake of this investigation, we have focused primarily on the Langmuir and Freundlich isotherms to examine

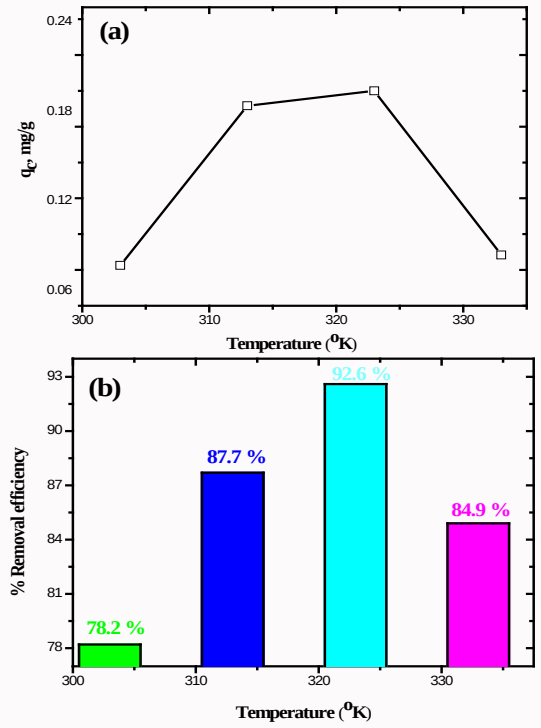

Figure 8: Effect of temperature on: (a) adsorption capacity (q_c) and (b) removal efficiency in 40 mg/l of dye using (Cu^{2+}-Az) complex.

the adsorption behavior of the adsorbent. In terms of the kind of adsorption behavior shown, the Langmuir isotherm demonstrates monolayer adsorption whereas the Freundlich isotherm demonstrates heterogeneous adsorption behavior [45]. It has been observed that the sorption capacity (q_m) was discovered to be (0.0061 mg/g) at 547 nm in Table 2. The fact that the correlation coefficient has such a high value (0.999) demonstrates that the Langmuir isotherm, which presumes a monolayer covering and a uniform activity distribution on the sorbent surface, may be used. The Freundlich isotherm model was also fit to the equilibrium data such that it would follow the model. The sorption capacity of the system was represented by the K_f constant, while the sorption intensity was represented by the n constant. The significance of the term (1/n) provides insight into the degree to which sorbent/adsorbate systems are likely to be successful [43,45-50].

Adsorption kinetics: The equation for the first-order rate is as follows:

$$\ln(q_c - q_t) = \ln q_c - K_1 t \quad (6)$$

Where q_c and q_t represent the amount of dye that was adsorbed on the sorbent at equilibrium and time t (mg/g), respectively and K_1 is the first-order rate constant (min^{-1}). The curvature line may be found by plotting $\ln(q_c - q_t)$ against time.

The expression for the linearized form of the first-order rate is as follows [51]:

$$\frac{dq_1}{dt} = k_2 (q_e - q_e)^2 \quad (7)$$

$$\frac{t}{q_t} = \frac{1}{k_2 q_e^2} + \frac{t}{q_e} \quad (8)$$

Where q_e is the quantity of adsorbate that is adsorbed by a sorbent for every unit mass when the system is in equilibrium (mg/g), q_t is the quantity of adsorbate that was adsorbed at the contact time t (mg/g), and k_2 is the pseudo-second-order rate constant (g/mg min). A linear connection is seen when t/qt is plotted against t; as a result, q_e and k_2 may be derived from the slope and intercept of the linear relationship. Because the correlation coefficient for a first-order kinetic model is 0.933, the experimental results for the adsorption of (NFD) on (Cu^{2+}-Az) complex were applied to fit first-order kinetic models with a correlation coefficient of 0.94. This is because the correlation coefficient in the case of a first-order kinetic model is 0.93. The results showed that the value of k_1 is (0.018) and adsorption process not obeyed second order. This demonstrated that chemisorption, which involves valence forces and involves the sharing or exchange of electrons, is the step that limits the reaction rate [52].

The equation that describes intraparticle diffusion may be written as follows:

$$q_t = K_d t^{1/2} + C \quad (9)$$

Where K_d is the constant that represents the intraparticle diffusion rate (mg/g $min^{1/2}$), based on the results of the experiments, the intraparticle diffusion rate is (3×10^{-4} mg/g $min^{1/2}$), the linear component of the plot does not go through the point of origin. This departure from the initial route is caused by the possibility of a fluctuating mass transfer rate throughout the early and end phases of the adsorption process. The fact that there was adsorption on the outside surface and diffusion into the inside of the (Cu^{2+}-Az) complex proves that (NFD) adsorption was a multi-step process. Adsorption occurred on the exterior surface, and diffusion occurred within [53].

Adsorption thermodynamics: The free energy change (ΔG^o), the enthalpy change (ΔH^o), and the entropy change (ΔS^o) are the thermodynamic parameters that were computed for the (NFD) adsorption onto the (Cu^{2+}-Az) complex. The following equation was used to get these values for the parameters [54-61].

$$\Delta G° = -2.303\ RT \log K_D \quad (10)$$

Where $K_D = q_c/C_e$

Also,

$$\Delta G° = \Delta H° - T\Delta S° \quad (11)$$

$$\ln K_D = \frac{\ddot{A}S^\circ}{R} - \frac{\Delta H^\circ}{RT} \quad (12)$$

Where q_e is the concentration of (NFD) at equilibrium onto the (Cu^{2+}-Az) complex (mg/L), R is universal gas constant (8.314 J/mol K), and C_e is the concentration of (NFD) at equilibrium in solution (mg/L). The values of H° and ΔS° were derived by analyzing the slope and intercept of the plot of ln K_D against 1/T. Gibbs free energy change of sorption, denoted as (ΔG°), was computed with the help of Equation (11).

The equations (10) through (12) were used to determine the values of the thermodynamic constants (ΔH°, ΔS° and ΔG°) for (NFD) adsorption. The values of ΔH° and ΔS° were derived from the slope and intercept of a plot comparing the ln of K_D against 1/T. Table 3 is an illustration of the thermodynamic parameters involved in the adsorption of (NFD) onto (Cu^{2+}-Az) complex. The positive value of ΔH° kJmol^{-1} indicates that the adsorption of (NFD) onto (Cu^{2+}-Az) complex is an endothermic reaction. The calculated negative value of ΔG° kJmol^{-1} indicates spontaneous nature of the adsorption

Table 3: Thermodynamic parameters values.

Parameter	ΔH°(kJmol^{-1})	ΔS° (Jmol^{-1}K^{-1})	ΔG° (kJmol^{-1})
*K_D (at λ_{max}=547 nm)	52.3782	186.5661	-4.1513

process. Further the value of entropy change, ΔS° J/molK reflects the non-affinity of (Cu^{2+}-Az) complex for (NFD) dye. The results are summarized in Table 3.

Conclusion

In this study, the removal of (NFD) dye from aqueous solutions was accomplished by effectively synthesizing a copper complex. Analyses conducted using UV-Vis, SEM, FTIR, and Mass were used to evaluate the produced (Cu^{2+}-Az). These tests revealed that the complex has outstanding surface chemistry in addition to excellent textural qualities (microporosity, large surface area, and granular morphology). The (Cu^{2+}-Az) complex dosage, the contact time, the concentration of (NFD) dye, and the temperature all have an effect on the adsorption process. The kinetic mechanism for first-order adsorption was the one that the adsorption process adhered to the most closely. The modeling of equilibrium isotherms demonstrated a strong correlation between the (NFD) adsorption onto (Cu^{2+}-Az) complex and the Langmuir model. It was shown that the highest capacity for absorption was 0.194 mg/g. The examination of the thermodynamic parameters unearthed the fact that the (NFD) dye adsorption process was an endothermic and spontaneous occurrence. This work showed that (Cu^{2+}-Az) complex might be utilized as a viable adsorbent to remove (NFD) dye from industrial effluents. In addition, it is a source that is inexpensive and widely available.

Acknowledgment

This work is supported by the Chemistry Department, Faculty of Science, New Valley University, El-Kharga 72511, New Valley, Egypt. The authors would like to thank all staff members of the Chemistry Department for their continuous encouragement of this scientific research.

References

1. Kolkaila SA, Ali AE, Elasala GS. Synthesis, spectral characterization of azithromycin with transition metals and a molecular approach for azithromycin with Zinc for COVID-19. Int J Cur Res Rev. 2021;13(23):53-9.
2. Parnham MJ, Haber VE, Giamarellos-Bourboulis EJ, Perletti G, Verleden GM, Vos R. Azithromycin: Mechanisms of action and their relevance for clinical applications. Pharmacol Ther. 2014;143(2):225-45.
3. Luo X, Hao T, Yue L, Hong G, Lu Y. Azithromycin wastewater treatment with La doping titanium dioxide/active carbon composites, 2015 4^{t}h International Conference on Sensors, Measurement and Intelligent Materials. Atlantis Press. 2016:861-70.
4. Echeverría-Esnal D, Martin-Ontiyuelo C, Navarrete-Rouco ME, De-Antonio Cusco M, Ferrández O, Horcajada JP, et al. Azithromycin in the treatment of COVID-19: A review. Expert Rev Anti Infect Ther. 2021;19(2):147-63.
5. Beigel JH, Tomashek KM, Dodd LE, Mehta AK, Zingman BS, Kalil AC, et al. Remdesivir for the treatment of COVID-19-Final report. N Engl J Med. 2020;383:1813-26.
6. Tasić ŽZ, Mihajlović MBP, Radovanović MB, Antonijević MM. Electrochemical investigations of copper corrosion inhibition by azithromycin in 0.9% NaCl. J Mol Liq. 2018;265:687-92.
7. Casey A, Adams D, Karpanen T, Lambert P, Cookson B, Nightingale P, et al. Role of copper in reducing hospital environment contamination. J Hosp Infect. 2010;74(1):72-7.
8. Mehtar S, Wiid I, Todorov S. The antimicrobial activity of copper and copper alloys against nosocomial pathogens and *Mycobacterium tuberculosis* isolated from healthcare facilities in the Western Cape: An *in-vitro* study. J Hosp Infect. 2008;68(1):45-51.
9. Sher A, Rau H, Greiner G, Haubold W. Spectroscopic and polarographic investigations of copper (II)-azithromycin interactions under equilibrium conditions. Int J Pharm. 1996;133:237-44.
10. El-Rjoob AW, Al-Mustafa J, Taha Z, Abous M. Spectroscopic and conductometric investigation of the interaction of azithromycin with iron (II) ion. Jordan J Chem. 2008;3(2):199-209.
11. Arayne S, Sultana N, Shamim S, Naz A. Synthesis characterization and antimicrobial activities of azithromycin metal complexes. Mod Chem Appl. 2014;2(3):1000133.
12. Saleh R, Taufik A. Degradation of methylene blue and Congo-red dyes using Fenton, photo-Fenton, Sono-Fenton, and Sonophoto-Fenton methods in the presence of iron (II, III) oxide/zinc oxide/graphene (Fe3O4/ZnO/graphene) composites. Sep Purif Technol. 2019;210:563-73.
13. Lam SM, Sin JC, Abdullah AZ, Mohamed AR. Degradation of wastewaters containing organic dyes photocatalyzed by zinc oxide: A review. Desalination Water Treatment. 2012;41(1-3):131-69.
14. Zhang Q, Peng Y, Deng F, Wang M, Chen D. Porous Z-scheme MnO2/Mn-modified alkalinized g-C3N4 heterojunction with excellent Fenton-like photocatalytic activity for efficient degradation of pharmaceutical pollutants. Sep Purif Technol. 2020;246:116890.
15. Talukdar S, Dutta RK. A mechanistic approach for superoxide radicals and singlet oxygen mediated enhanced photocatalytic dye degradation by selenium doped ZnS nanoparticles. RSC Adv. 2016;6:928-36.
16. Hunger K. Industrial dyes: Chemistry, properties, applications. John Wiley & Sons, 2007.
17. Ong ST, Tan SY, Khoo EC, Lee SL, Ha ST. Equilibrium studies for Basic blue 3 adsorption onto durian peel (Durio Zibethinus Murray). Desalination Water Treatment. 2012;45(1-3):161-9.
18. Ghoniem MG, Ali FAM, Abdulkhair BY, Elamin MRA, Alqahtani AM, Rahali S, et al. Highly selective removal of cationic dyes from wastewater by MgO nanorods. Nanomater. 2022;12:1023.
19. Haddad ME. Removal of basic fuchsin dye from water using mussel shell biomass waste as an adsorbent: Equilibrium, kinetics, and thermodynamics. J Taibah University Sci. 2016;10:664-74.
20. Georgin J, Franco D, Drumm FC, Grassi P, Netto MS, Allasia D, et al. Powdered biosorbent from the mandacaru cactus (*Cereus jamacaru*) for discontinuous and continuous removal of Basic Fuchsin from aqueous solutions. Powder Technol. 2020;364:584-92.
21. Santos ABD, Cervantes FJ, Lier JBV. Review paper on current technologies for decolorization of textile wastewaters: Perspectives for anaerobic biotechnology. Bioresour Technol. 2007;98(12):2369-85.
22. Anfar Z, Amedlous A, Fakir AAE, Ahsaine HA, Zbair M, Lhanafi S, et al. Combined methane energy recovery and toxic dye removal by porous carbon derived from anaerobically modified digestate. ACS Omega. 2019;4(5):9434-45.
23. Anfar Z, Ahsaine HA, Zbair M, Amedlous A, Fakir AAE, Jada A, et al. Recent trends on numerical investigations of response surface methodology for pollutants adsorption onto activated carbon materials: A review. Crit Rev Environ Sci Technol. 2020;50(10):1043-84.
24. Anfar Z, Amedlous A, El Fakir AA, Zbair M, Ahsaine HA, Jada A, et al. High extent mass recovery of alginate hydrogel beads network based on immobilized bio-sourced porous carbon@ Fe3O4-NPs for organic pollutants uptake. Chemosphere. 2019;236:124351.
25. Esplugas S, Bila DM, Krause LGT, Dezotti M. Ozonation and advanced

oxidation technologies to remove endocrine disrupting chemicals (EDCs) and pharmaceuticals and Personal Care Products (PPCPs) in water effluents. J hazard mater. 2007;149(3):631-42.

26. Saratale RG, Saratale GD, Chang JS, Govindwar SP. Bacterial decolorization and degradation of azo dyes: A review. J Taiwan Inst Chem Eng. 2011;42(1):138-57.

27. El Fakir AA, Anfar Z, Amedlous A, Zbair M, Hafidi Z, El Achouri M, et al. Engineering of new hydrogel beads based conducting polymers: Metal-free catalysis for highly organic pollutants degradation. Appl Catalysis B: Environ. 2021;286:119948.

28. Gupta V, Mittal A, Gajbe V, Mittal J. Adsorption of basic fuchsin using waste materials-bottom ash and deoiled soya-as adsorbents. J Colloid Interface Sci. 2008;319(1):30-9.

29. Jain SN, Gogate PR. Efficient removal of Acid Green 25 dye from wastewater using activated Prunus Dulcis as biosorbent: Batch and column studies. J Environ Manage. 2018;210:226-38.

30. Sriram G, Uthappa U, Rego RM, Kigga M, Kumeria T, Jung HY, et al. Ceria decorated porous diatom-xerogel as an effective adsorbent for the efficient removal of Eriochrome Black T. Chemosphere. 2020;238:124692.

31. Mohamed NS, Ibrahim SM, Ahmed MM, Al-Hossainy AF. Removal of toxic basic fuchsin dye from liquids by antibiotic azithromycin using adsorption, TD-DFT calculations, kinetic, and equilibrium studies§ . Ind Eng Chem Res. 2023;62(10):4312-27.

32. Al-Noor TH. Synthesis and Characterization of metal complexes with ligands containing a hetero (N) atom and (hydroxyl or carboxyl) group. Int J Sci Technol. 2012;7:2.

33. Ibrahim SM, Saad N, Ahmed MM, Abd El-Aal M. Novel synthesis of antibacterial pyrone derivatives using kinetics and mechanism of oxidation of azithromycin by alkaline permanganate. Bioorg Chem. 2022;119:105553.

34. Al-Noor TH, Jarad AJ, Hussein AO. Synthesis, Physico-chemical and antimicrobial properties of some metal (II)-mixed ligand complexes of tridentate Schiff base derives from B-Lactam antibiotic {(cephalexin mono hydrate)-4-chlorobenzophenone} and saccharin. Int J Chem Process Eng Res. 2014;1:109-20.

35. Watt GW, Chrisp JD. Spectrophotometric method for determination of hydrazine. Anal Chem. 1952;24(12):2006-8.

36. Khalid L, Mahsood N, Ali. The public health problem of OTC antibiotics in developing nations. Res Social Adm Pharm. 2016;12(5):801-2.

37. Ribeiro-Claro PJ, Vaz PD, Nolasco M. Crystal structure landscapes from combined vibrational spectroscopy and ab initio calculations: 4-(Dimethylamino) benzaldehyde. J Mol Struc. 2010;946(1-3):65-9.

38. Abdel Ghafar HH, Ali GA, Fouad OA, Makhlouf SA. Enhancement of adsorption efficiency of methylene blue on Co3O4/SiO2 nanocomposite. Desalination Water Treatment. 2015;53(11):2980-9.

39. Lo SF, Wang SY, Tsai MJ, Lin LD. Adsorption capacity and removal efficiency of heavy metal ions by Moso and Ma bamboo activated carbons. Chem Eng Res Des. 2012;90:1397-406.

40. El-Gamal S, Amin M, Ahmed M. Removal of methyl orange and bromophenol blue dyes from aqueous solution using Sorel's cement nanoparticles. J Environ Sci Eng. 2015;3:1702-12.

41. Yagub MT, Sen TK, Afroze S, Ang HM. Dye and its removal from aqueous solution by adsorption: A review. Adv Colloid Interface Sci. 2014;209:172-84.

42. Özacar M, Şengil İA. Adsorption of acid dyes from aqueous solutions by calcined alunite and granular activated carbon. Adsorption. 2002;8:301-8.

43. Malik PK. Use of activated carbons prepared from sawdust and rice-husk for adsorption of acid dyes: A case study of Acid Yellow 36. Dyes Pigments. 2003;56(3):239-49.

44. Tharaneedhar V, Kumar PS, Saravanan A, Ravikumar C, Jaikumar V. Prediction and interpretation of adsorption parameters for the sequestration of methylene blue dye from aqueous solution using microwave assisted corncob activated carbon. Sustainable Material Technol. 2017;11:1-11.

45. Al-Aoh HA. Adsorption performances of Nickel Oxide Nanoparticles (NiO NPs) towards bromophenol Blue Dye (BB). Desalin Water Treat. 2018;110:229-38.

46. Liang S, Guo X, Feng N, Tian Q. Isotherms, kinetics and thermodynamic studies of adsorption of Cu2+ from aqueous solutions by Mg2+/K+ type orange peel adsorbents. J Hazard Mater. 2010;174:756-62.

47. Ibrahim SM, Al-Hossainy AF. Synthesis, structural characterization, DFT, kinetics and mechanism of oxidation of bromothymol blue: Application to textile industrial wastewater treatment. Chem Papers. 2021;75:297-309.

48. Al-Hossainy AF, Ibrahim SM. Oxidation process and kinetics of bromothymol blue by alkaline permanganate. Int J Chem Kinet. 2021;53(5):675-84.

49. Al-Hossainy AF, Ibrahim A, Mogharbel RT, Ibrahim SM. Synthesis of novel keto-bromothymol blue in different media using oxidation–reduction reactions: Combined experimental and DFT-TDDFT computational studies. Chem Papers. 2021;75:3103-18.

50. Akbari A, Sabouri Z, Hosseini HA, Hashemzadeh A, Khatami M, Darroudi M. Effect of nickel oxide nanoparticles as a photocatalyst in dyes degradation and evaluation of effective parameters in their removal from aqueous environments. Inorganic Chem Commun. 2020;115:107867.

51. Ho Y, McKay G, Wase D, Forster C. Study of the sorption of divalent metal ions on to peat. Adsorption Sci Technol. 2000;18(7):639-50.

52. Bhattacharyya KG, Sharma A. Kinetics and thermodynamics of methylene blue adsorption on neem (*Azadirachta indica*) leaf powder. Dyes Pigments. 2005;65(1):51-9.

53. Kumar KV, Kumaran A. Removal of methylene blue by mango seed kernel powder. Biochem Eng J. 2005;27(1):83-93.

54. Hassan R, Ibrahim S, Zaafarany I, Fawzy A, Takagi H. Base-catalyzed oxidation: Kinetics and mechanism of hexacyanoferrate (III) oxidation of methyl cellulose polysaccharide in alkaline solutions. J Mol Catal A Chem. 2011;344(1-2):93-8.

55. Hassan RM, Ibrahim SM. Oxidation of some sustainable sulfated natural polymers: Kinetics and mechanism of oxidation of water-soluble chondroitin-4-sulfate polysaccharide by hexachloroiridate (IV) in aqueous solutions. ACS Omega. 2019;4:2463-71.

56. Hassan RM, Ibrahim SM. Base-catalyzed oxidation of sulfated kappa-carrageenan by alkaline hexacyanoferrate (III): A mechanistic approach of electron-transfer process. J Mol Liq. 2019;273:177-82.

57. Hassan R, Takagi H, Ibrahim S. Orientation on the Mechanistics of electron-transfer on oxidation of chondroitin-4-sulfate as sustainable sulfated polysaccharide by permanganate ion in aqueous perchlorate solutions. J Renew Mater. 2020;8(2):205-18.

58. Hassan RM, Ibrahim SM, Takagi HD, Sayed SA. Kinetics of corrosion inhibition of aluminum in acidic media by water-soluble natural polymeric chondroitin-4-sulfate as anionic polyelectrolyte inhibitor. Carbohydr Polym. 2018;192:356-63.

59. Hassan R, Ibrahim S, Salman S, Takagi H. A promising water-soluble synthetic polymer of high efficiency and low cost as inhibitor for inhibition of metals corrosion: Inhibition of magnesium corrosion by poly (ethylene glycol) in acidic media. J Bio Tribocorros. 2019;5:1-10.

60. Ibrahim SM, Althagafi I, Takagi HD, Hassan RM. Kinetics and mechanism of oxidation of chondroitin-4-sulfate polysaccharide as a sulfated polysaccharide by hexacyanoferrate (III) in alkaline solutions with synthesis of novel coordination biopolymer chelating agent. J Mol Liq. 2017;244:353-9.

61. Ibrahim SM, Al-Hossainy AF. Kinetics and mechanism of oxidation of bromothymol blue by permanganate ion in acidic medium: Application to textile industrial wastewater treatment. J Mol Liq. 2020;318:114041.